Supplementary Materials 1 for

Structural Evaluation of Interleukin-19 Cytokine and Interleukin-19-Bound Receptor Complex Using Computational Immuno-Engineering Approach

Urmi Roy

Department of Chemistry & Biochemistry, Clarkson University, 8 Clarkson Avenue, Potsdam, NY 13699, USA; urmi@clarkson.edu

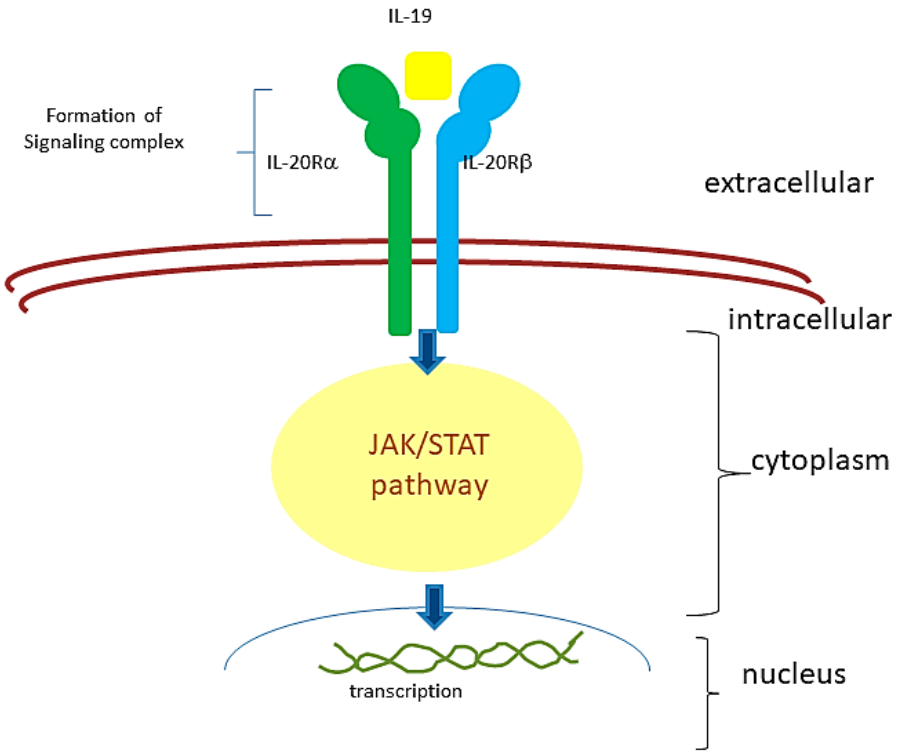

Figure S1. Schematic illustration of IL-19/IL-20R pathway. This figure is based on general concept.

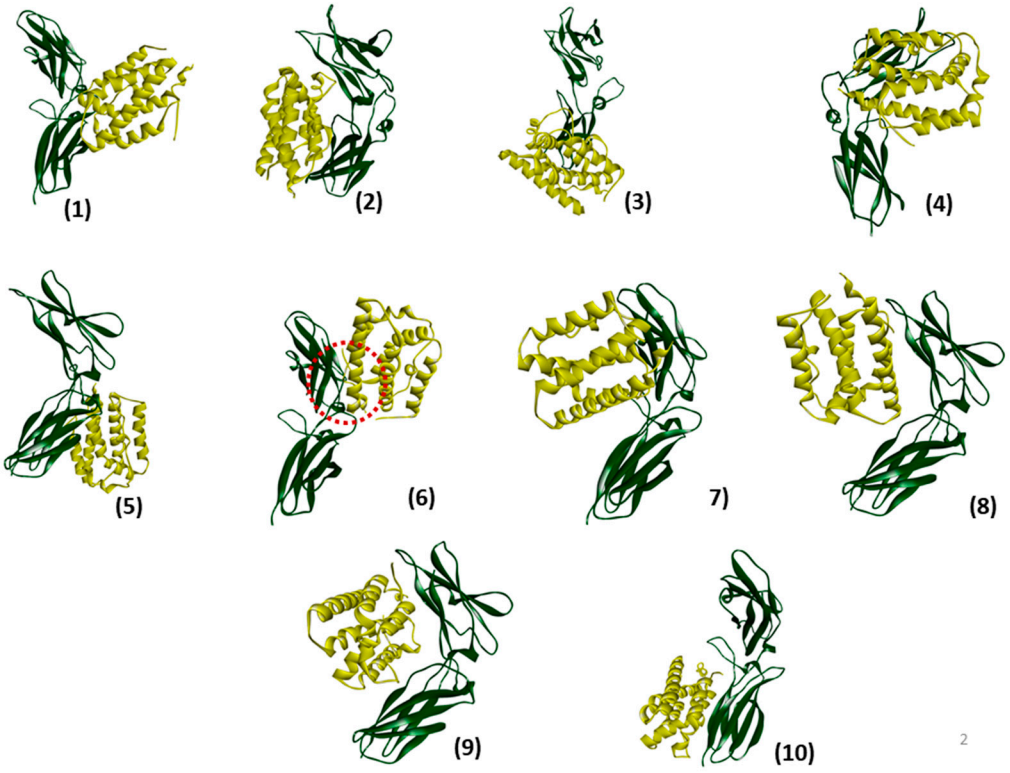

Figure S2. This figure represents the first docking experiment of Figure 3, Scheme 1, the predicted structural models of IL-19 (1N1F, yellow) bound IL-20 alphaR receptor (4DOH: Chain R; green). These models are predicted using GrammX server. Model 6 was selected for second set of docking experiment of Scheme 1. Visual inspection reveals that Model 6 has similarity with 4DOH.PDB. The interface area αR:A in model

6 is 758.4 Å^2.The solvation free energy gain upon formation of the interface R:A in model 6 is -8.3 kcal/mol. This calculation was done by PDBePISA.

Here in most cases, the ligands did not bind to the proper binding region. In some cases the ligand has flipped its orientation compare to 4DOH.PDB. In all docking experiments the blind docking method was used without specifying the target-binding site.

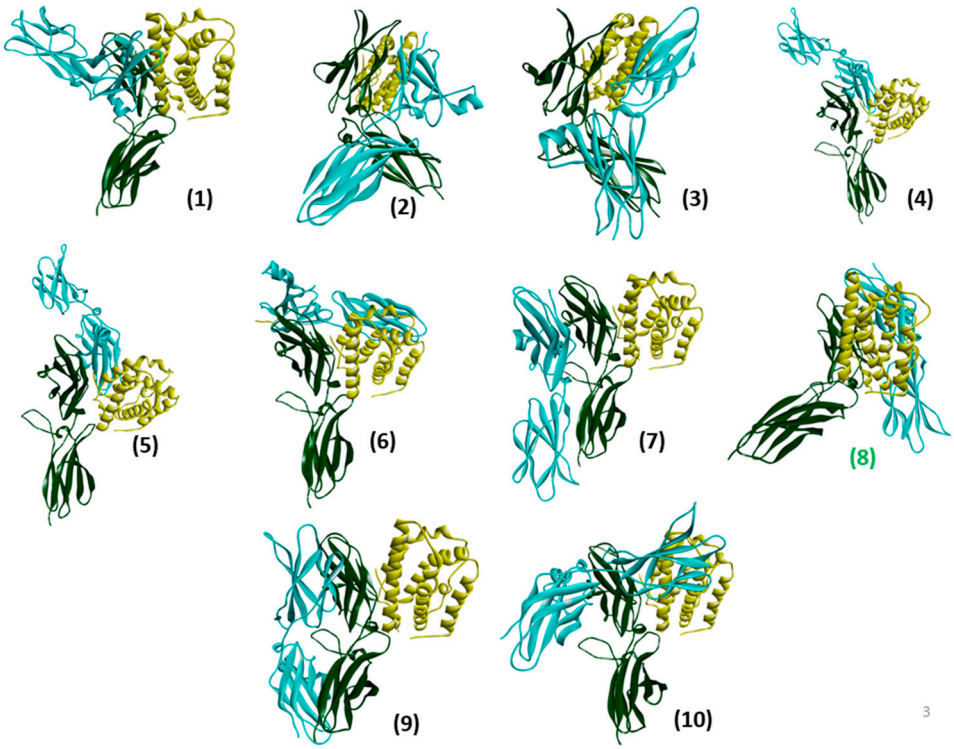

Figure S3. This figure represents the second set of docking mentioned in Figure 3; Scheme 1. This figure is a continuation of previous Figure, Figure S2. These models are predicted binding between previous model (model 6, Figure S2) & 4DOH: beta B (IL-20R2; cyan).

Although the model 8 visually looks similar, a closer look (binding residue analyses) reveals that the ligand binds mostly to the opposite binding site of beta chain as compared to 4DOH. Therefore no model was selected from Figure3 Scheme 1 for further analyses.

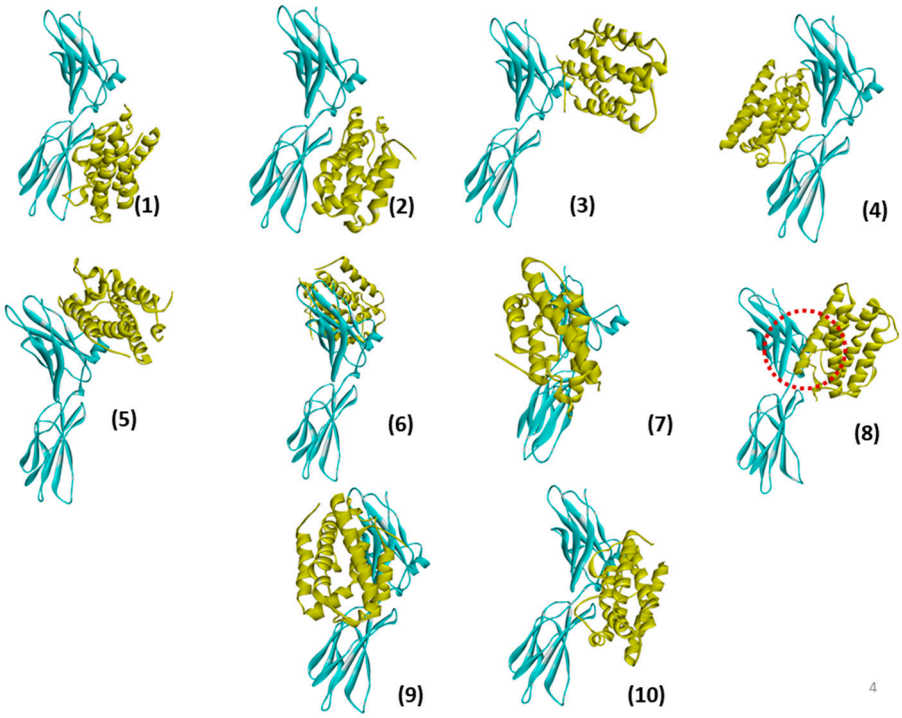

Figure S4. This figure represents the first set of docking experiment in Figure 3, Scheme 2. These models are predicted using GrammX server. These structures are predicted bindings between IL-19 (1N1F; yellow) and IL-20 betaB receptor (4DOH: chain B; cyan). Model 8 was selected for further studies.

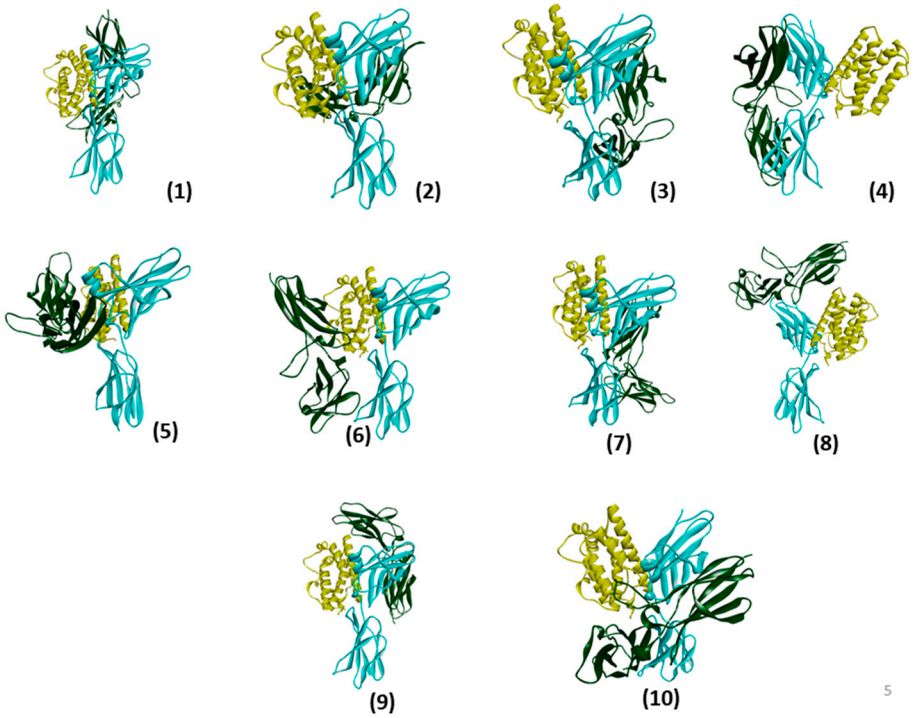

Figure S5. This figure represents the second set of docking in Figure 3, Scheme 2. This figure is a continuation of Figure S4. These models are predicted using GrammX server. Predicted binding of model 8 (IL-19 bound IL-20B beta, from Figure S4) and IL-20R alpha. As we did not get any suitable model, we did not proceed further using this scheme.

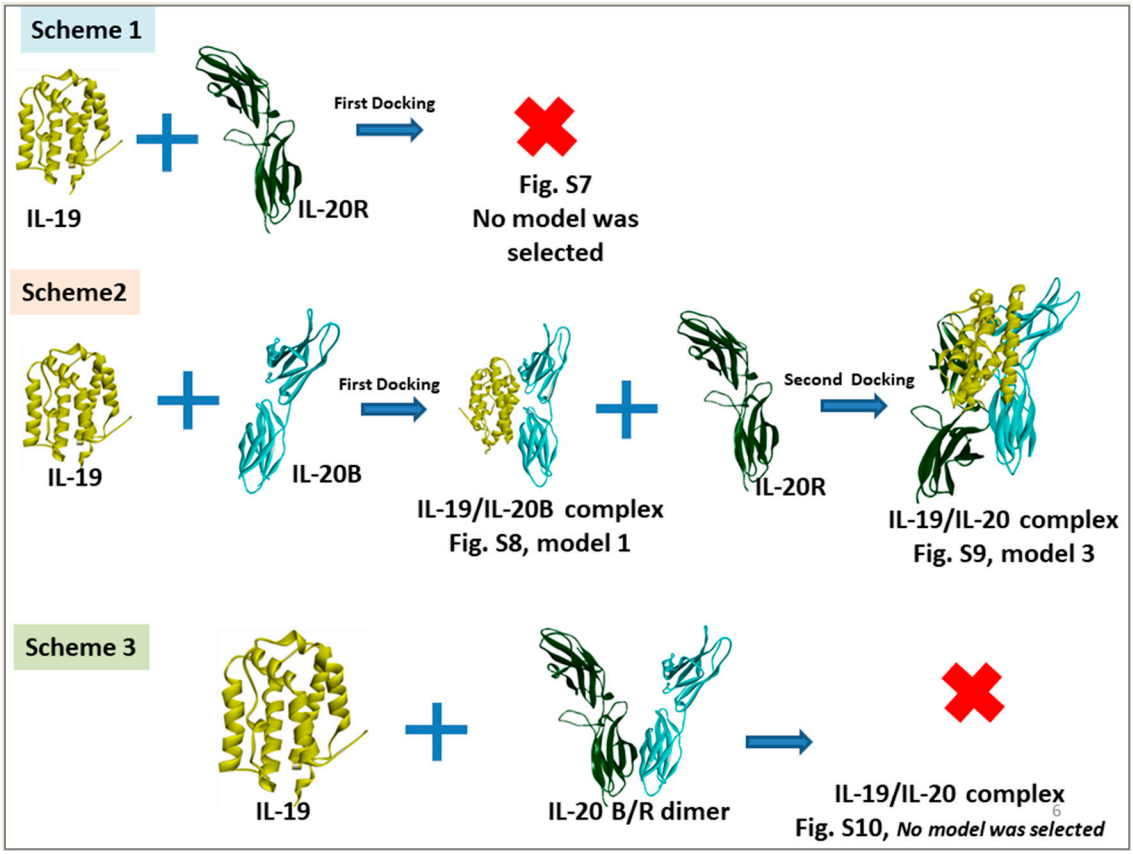

Figure S6. Predicted structure-based model of IL-19 bound IL-20 receptors using PatchDock/FireDock server. Firedock ranks the models based on binding energy. **Scheme 1** Prediction of IL-19 bound IL-20 alpha R and IL-20 beta B complex. No model was selected from this scheme for further study (Figure S7). **Scheme 2.** IL-19 bound IL-20 betaB/alpha R complex. Model 3 was selected from this scheme (Figures S8 and S9). This final model is considered as model B. **Scheme 3.** Binding of IL-19 to IL-20 dimer (IL-20 beta B/alpha R complex). No model was selected from this scheme for further study (Figure S10).

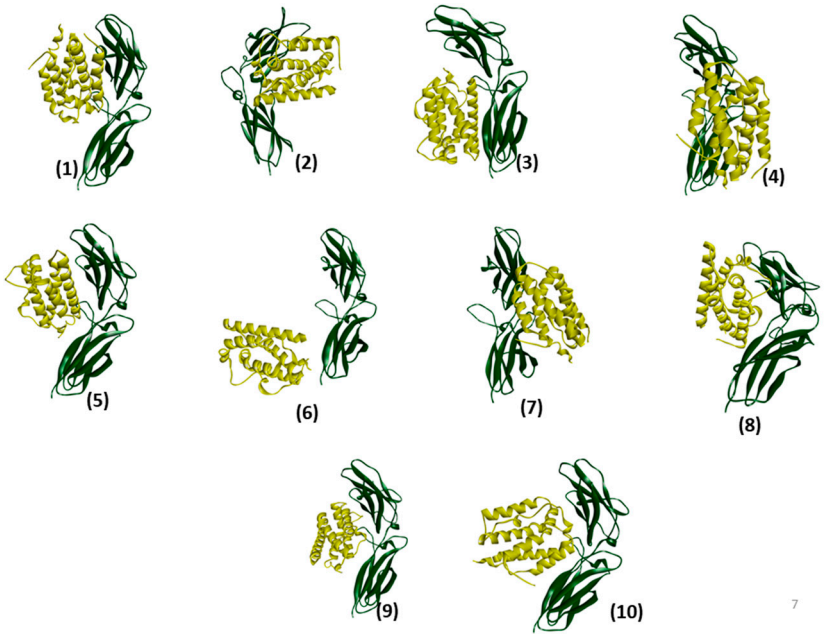

Figure S7. This figure represents the first set of docking displayed Figure S6, Scheme 1. These models are predicted using PatchDock/Firedock server. Predicted are the structural models of IL-19(1N1F) bound IL-20 alpha R receptor (4DOH: chain A; green).

No model was selected for further studies. Here in most cases, the ligand bound to receptor in flipped orientation, in some cases, the ligand binds to the D2 subunit of alpha R receptor. No model from Figure S7 was selected for further studies.

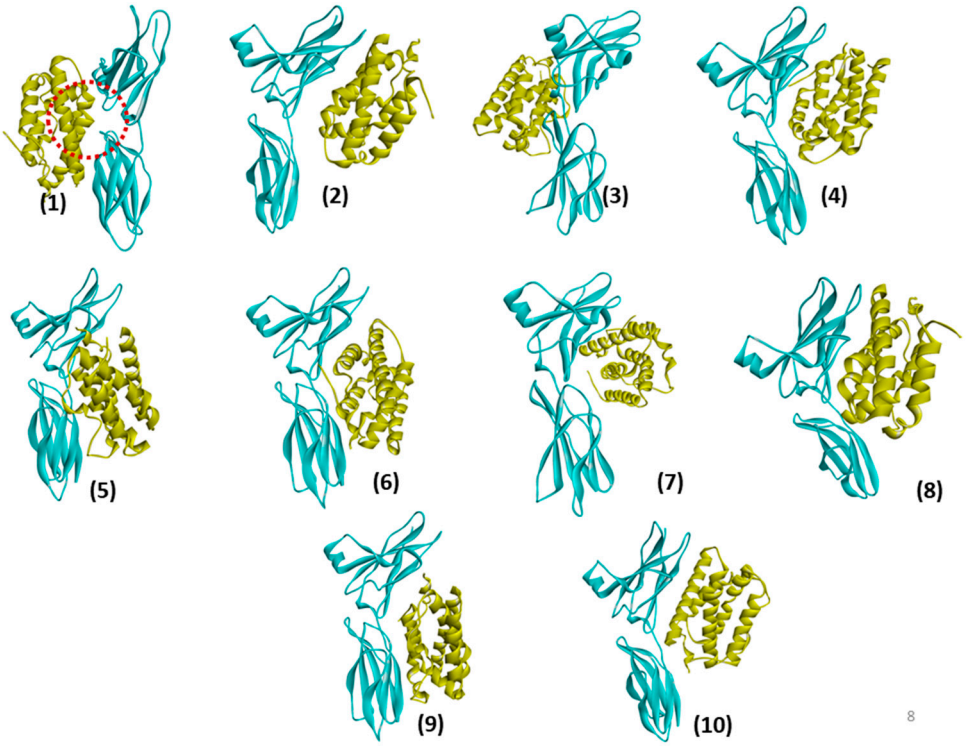

Figure S8. This figure represents the first docking of FigureS6, Scheme 2. Predicted structural models of IL-19 (1N1F) bound IL-20 beta B (DOH: chain B; cyan) receptor. Model 1 was selected for further studies (PatchDock/FireDock global energy: -22.23 energy unit). Here models 1-3 have the negative global energy. The lower global energy denotes favorable ligand–receptor interactions. The interfacial area of βB:A in model 1 is 1074.0Å^2. The solvation free energy gain upon formation of the interface βB:A in model 1 is -8.7 kcal/mol. This calculation was done by PDBePISA.

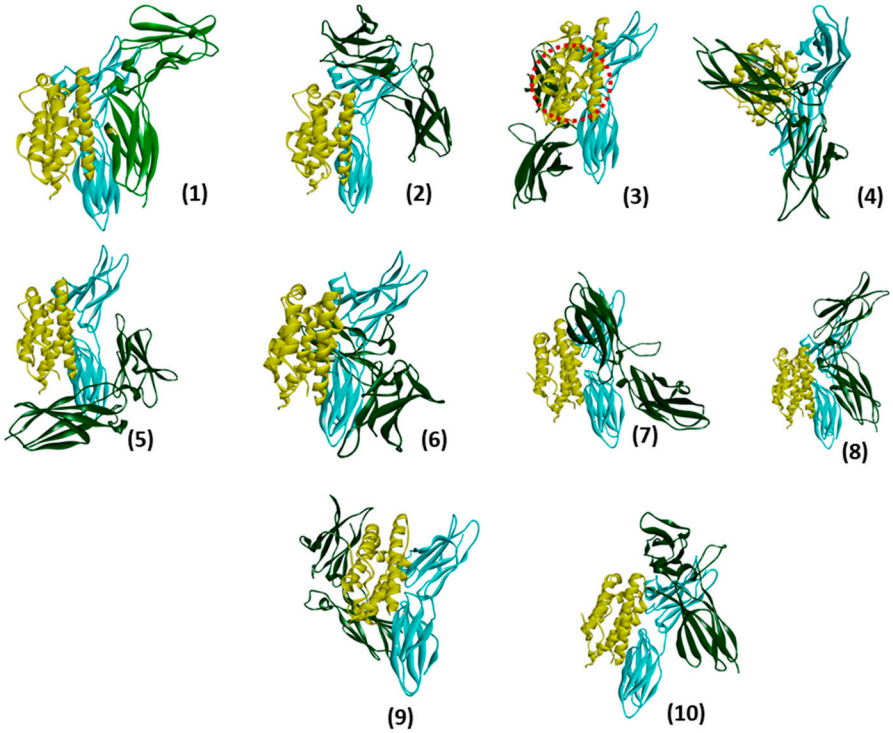

Figure S9. This figure represents the second docking of Figure S6, Scheme 2. This figure is a continuation of Figure S8. This figure displays the predicted binding between previous model (model 1 of Figure S8) & IL-20 alpha R receptor (4DOH: chain R; green). Visual assessment revels that some of these models form nonspecific binding. In some cases, the ligand binds to the D2 domain of the receptor and/or binds one of the two receptors. Additionally, in this docking experiment, models 1-6 have negative binding energy.

Although not entirely adequate, structural model 3 (PatchDock/FireDock global energy: -13.50 energy unit) is finally selected for further analyses as this model behaves mostly in expected way. The negative energy denotes stronger and better binding. This model is considered as model B. However, in case of model B the neighboring residues of the ligand mostly include the residues from the D2 subunits of alpha R and beta B. The interfacial region between subunits βB: A, αR: A and αR: βB within model B are 1076.6 $Å^2$, 650.6 $Å^2$ and 518.8 $Å^2$ respectively. The solvation free energy gain (kcal/mol) due to the formation of interfaces between βB: A, αR: A and αR: βB are -8.7, -1.8 and -4.6 respectively. This calculation was done by PDBePISA.

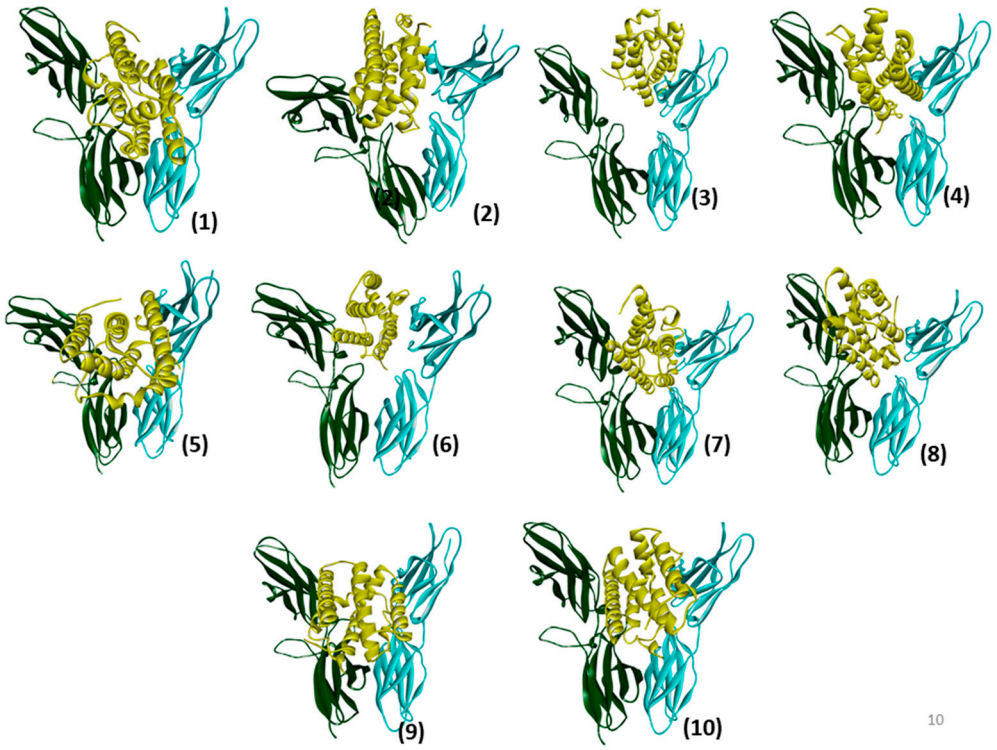

Figure S10. This figure represents Figure S6, Scheme 3. Predicted Structural Models of IL-19 bound IL-20 hetero-dimeric receptor. Predicted bindings between IL-19 (1N1F) and IL-20 alphaR (4DOH: chain A; green) and IL-20 betaB (4DOH: chain B; cyan). In model 1 and 2, the ligand is in flipped configuration. In model 3 the ligand is bound to beta receptor. In model 5, the ligand is flipped and also binds to the lower part (D2) of the receptor dimer. In model 7 and 8 the ligand is slightly flipped. Though models 4, 6, 9 and 10 are visibly look appropriate, from model 4 and onwards the global energy is positive. The positive global energy denotes unfavorable ligand–receptor interactions. Therefore, though binding pocket is similar in almost all cases, no model was selected for further studies.

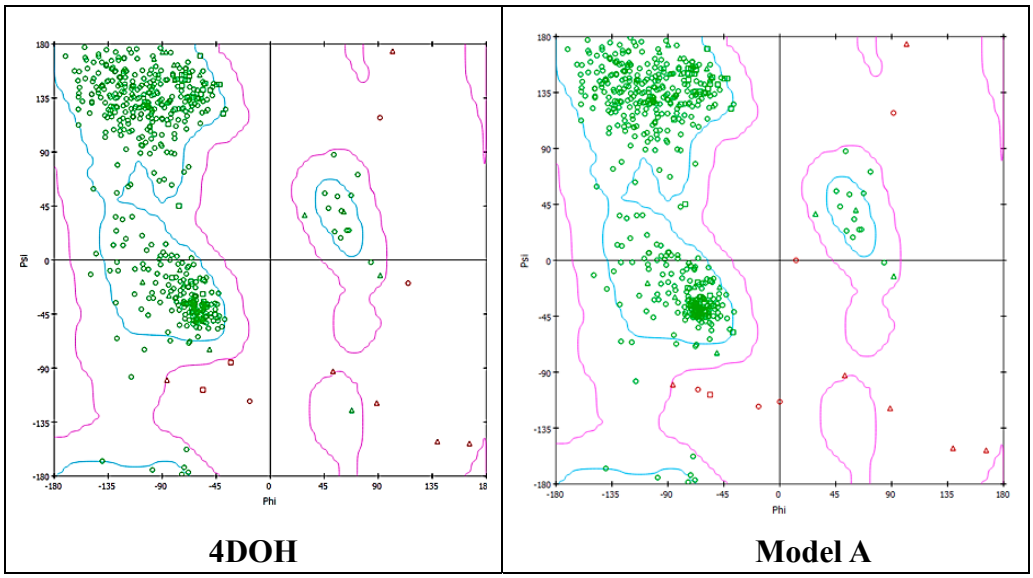

Figure S11. Ramachandran plots for 4DOH and model A. Default colors codes (Biovia's DSV) are used; cyan and violet boundaries denote the best and allowable regions. The white area denotes steric collisions and is only allowed for glycine (red triangles) and proline (red square).

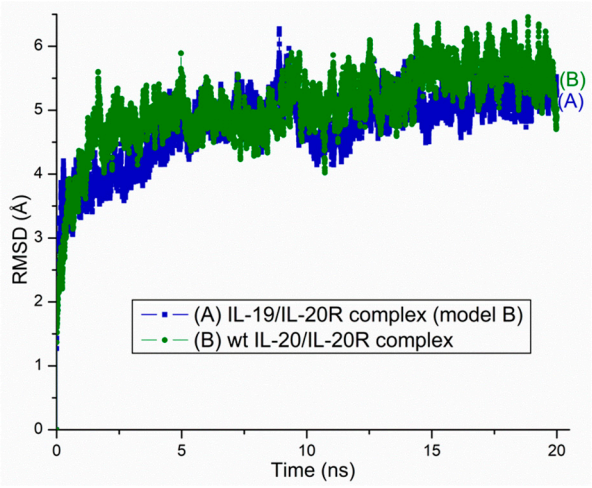

Figure S12. RMSD plots of wt IL-20/IL-20αRβB complex (4DOH.PDB, green) and the PatchDock/Firedock model B (Figure S6: Scheme 2; Figure S9: model 3; blue).

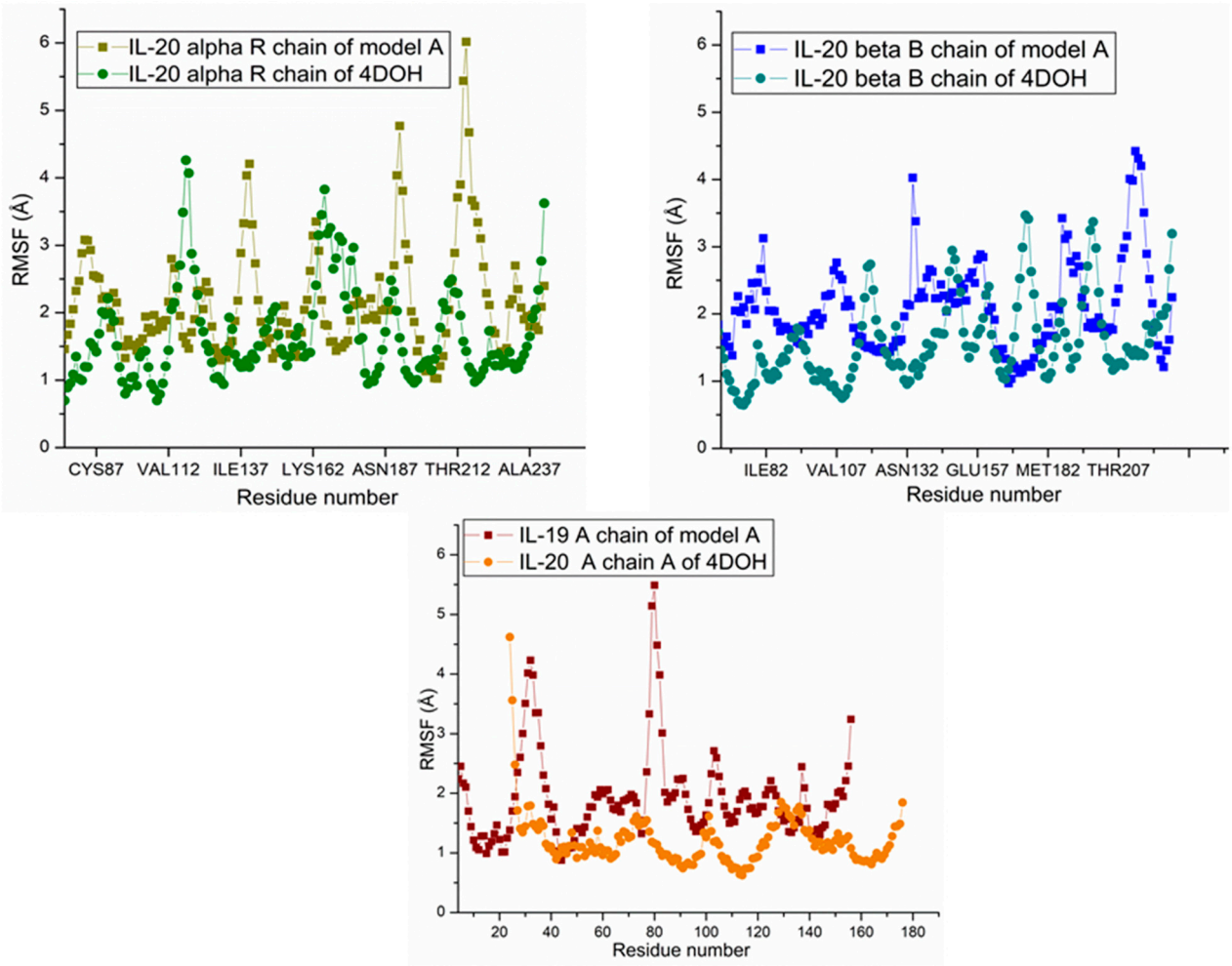

Figure S13. Comparative RMSF plots of 4DOH and model A. Here the root means square fluctuations are plotted as functions of residue numbers. These plots compliment the RMSD plots. In this plots the fluctuations due to the some sequences presented in Table S2 can be identified.



Figure S14. Time based secondary structures of A. IL-20/IL-20R wt protein, 4DOH; and B. Model B (Patchdock/Firedock model; Figure S6 scheme 2; Figure S9, model 3). C. The scheme of the color codes used in this figure and elsewhere. The default color codes of VMD secondary structure analysis are used.

Table S1: Sequence Alignment of IL-19 and IL-20

A. Sequence Alignment of IL-19 (human; uniprot Id Q9UHD0) and B. IL-20 (human; uniprot Id Q9NYY1

This analysis was done by CLUSTAL O (1.2.4).

- /*/:/. indicate gaps/identical residues /conserved and semi-conserved substitutions.

```
sp|Q9UHD0-1|IL19_HUMAN      MKLQ----------CVSLWLLGTILILCSVDNHGLRRCLISTDMHHIEESFQEIKRAIQA     50
sp|Q9NYY1-1|IL20_HUMAN      MKASSLAFSLLSAAFYLLWTPS-----TGLKTLNLGSCVIATNLQEIRNGFSEIRGSVQA     55
                            ** .             **  .      .:.. .*  *:*:*:::.*.:.*.**: ::**

sp|Q9UHD0-1|IL19_HUMAN      KDTFPNVTILSTLETLQIIKPLDVCCVTKNLLAFYVDRVFKDHQEPNPKILRKISSIANS     110
sp|Q9NYY1-1|IL20_HUMAN      KDGNIDIRILRRTESLQDTKPANRCCLLRHLLRLYLDRVFKNYQTPDHYTLRKISSLANS     115
                            **   :: **   *:**  ** : **: ::** :*:*****::* *:   ******:***

sp|Q9UHD0-1|IL19_HUMAN      FLYMQKTLRQCQEQRQCHCRQEATNATRVIHDNYDQLEVHAAAIKSLGELDVFLAWINKN     170
sp|Q9NYY1-1|IL20_HUMAN      FLTIKKDLRLCHAHMTCHCGEEAMKKYSQILSHFEKLEPQAAVVKALGELDILLQWMEET     175
                            ** ::* ** *: :  *** :** :    * .::::** :**.:*:*****::* *::::.

sp|Q9UHD0-1|IL19_HUMAN      HEVMFSA        177
sp|Q9NYY1-1|IL20_HUMAN      E------        176                                  .
```

B. Clustal Highlights

The clustal default color scheme is used here.

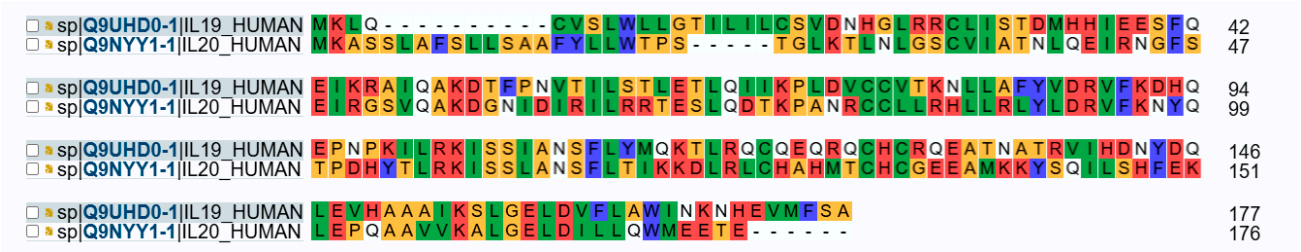

Physical Properties

C. Alignment of IL-19 and IL-20 based on *hydrophobicity*

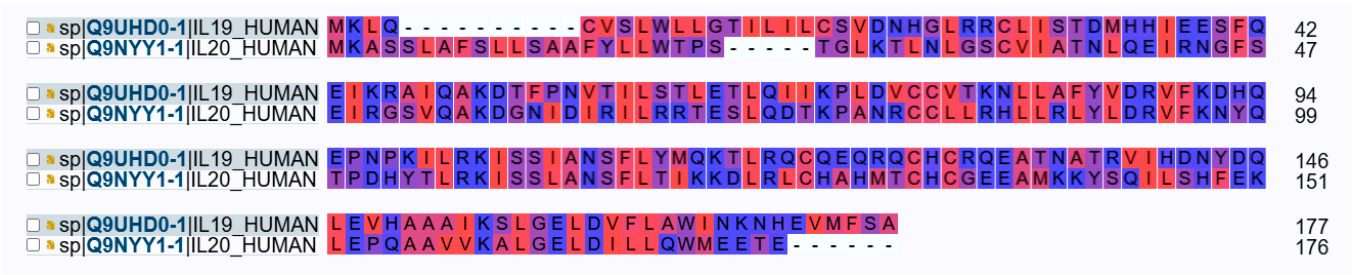

Structural Properties

D. Alignment of IL-19 and IL-20 based on *buried index*



E. Alignment of I-L19 and IL-20 based on *helix* propensity



F. Alignment of IL-19 and IL-20 based on *strand* propensity



G. Alignment of IL-19 and IL-20 based on *turn* propensity

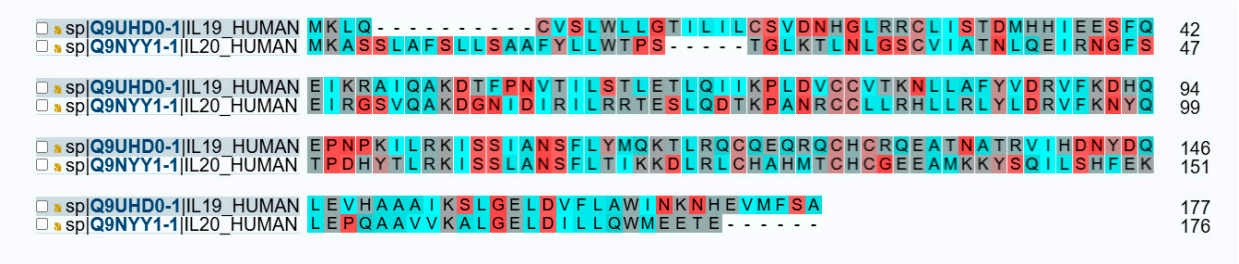

Table S2: List of subunit interface residues within 4DOH.PDB and model A

(*The interfacial residues of chains* IL-20αR and IL-20βB *are similar in two structures hence are not included.* For 4DOH the ligand is IL-20 and for model A the ligand is IL-19).

Subunit –interface	**4DOH** 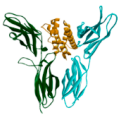	**Model A (GrammX model 1)** 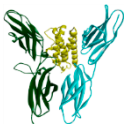
Interfacial residues of chain A (ligand IL-20/ligand IL-19): chain αR (receptor IL-20αR)	Gln40, Arg43, Asn44, Ser47, Gln54, Asp57, Asn59, Ile60, Asp61, Ile62, Arg63, Arg67, Lys160, Gly163, Glu164, Asp166, Ile167 and Gln170.	Met16, His17, Glu20, Glu21, Gln24, Lys27, Gln31, Asp34, Pro37, Asn38, Val39, Thr40, ILE41, Glu46, Leu48, Lys137, Gly140, Glu141, Asp143, Val144, Ala147, Lys151, Ser157 and Ala159.
Interfacial residues of chain A (ligand IL-20/ligand IL-19): chain βB (receptor IL-20βB)	Ala24, Leu25, Asn38, Gln40, Glu41, Leu91, Asp92, Phe95, Lys96, His103, Arg107, Ser110, Ser111, Ala113, Asn114, Ser115, Leu117, Thr118 and Lys121.	Asp15, His18, Val68, Phe72, Lys73, Pro80, Leu83, Arg84, Lys85, Ser87, Ser88, Asn91 and Ser158.
Interfacial residues of chain αR (receptor IL-20αR): chain A (ligand IL 20/ligand IL-19)	Phe74, Thr76, Gly77, Gln78, Lys79, Trp81, Asp103, Glu105, His106, Gln107, Tyr109, Glu125, Arg128, Tyr130, Phe132, Leu 133, Gly224, Pro225 and Pro226.	Phe74, Thr76, Gly77, Gln78, Lys79, Glu105, His106, Gln107, Arg128, Tyr130, Leu 133, Glu134, Phe221, Pro223, Gly224, Pro225 and Pro226.
Interfacial residues of chain βB (receptor IL-20βB): chain A (ligand IL 20/ligand IL-19)	TYR70, Gly72, Glu73, Tyr74, Glu75, Leu77, Tyr78, Thr79, Ile84, Pro85, Ser86, Ser87, Asp102, Thr104, Ala105, Thr106, Val107, Pro108, Tyr109, Arg133, Gln162, Glu164, Lys210 and Ala211.	TYR70, Tyr74, Glu75, Tyr78, Ile84, Pro85, Ser87, Asp101, Asp102, Thr104, Ala105, Thr106, Val107, Arg133, Arg184 and Lys210

Table S3: The hypothetical interacting area within the model structure A

The interfacial residues of chains IL-20αR *and* IL-20βB *are similar in 4DOH.PDB and Model 1 and hence are not included here.*

 **Residues of chain A (Ligand IL-19) close to chain αR (receptor IL-20αR)**	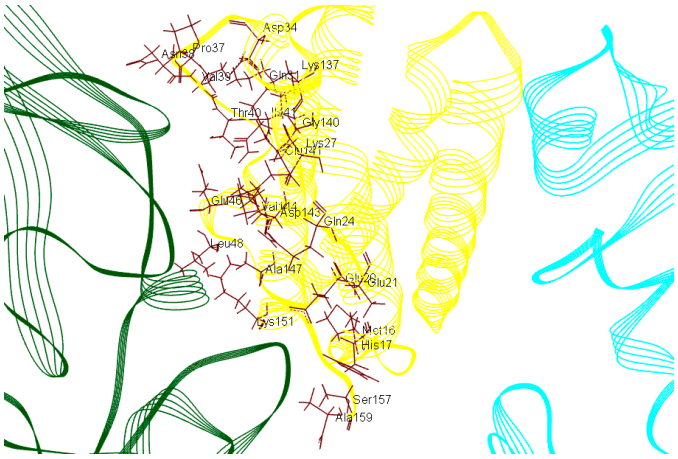 **Zoomed in view of chain A (Ligand IL-19) close to chain αR (receptor IL-20αR)**
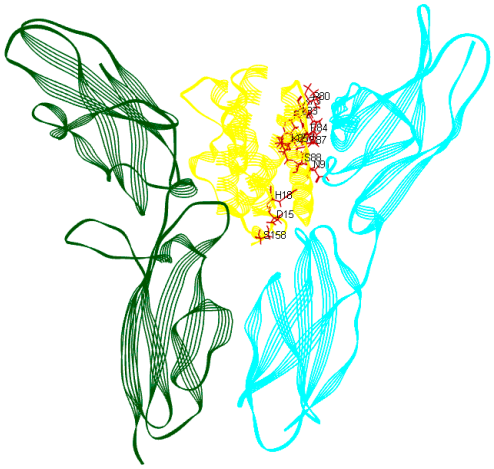 **Residues of chain A (Ligand IL-19) close to βB (receptor IL-20βB)**	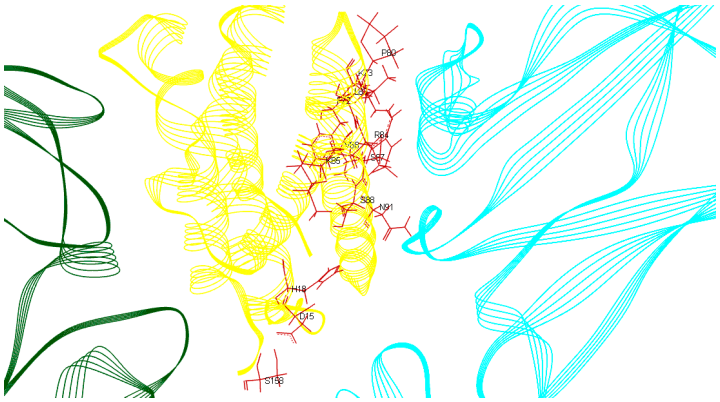 **Z oomed in view of residues of chain A (Ligand IL-19) close to chain βB (receptor IL-20βB)**
 **Residues of chain αR (receptor IL-20αR) close to chain A (ligand IL -19)**	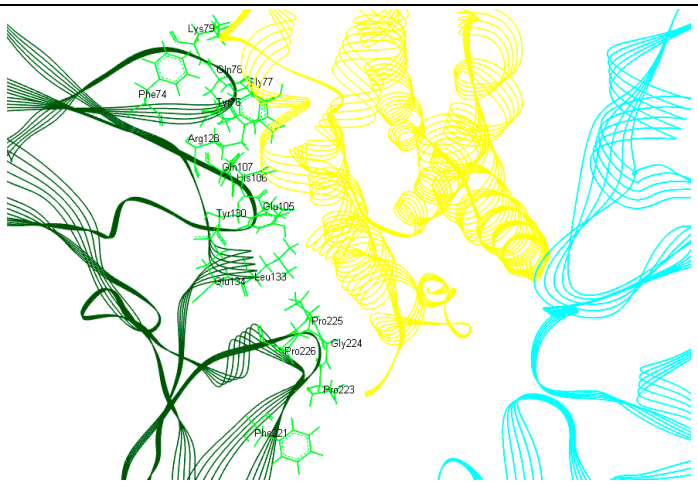 **Zoomed in view of residues of chain αR (receptor IL-20αR) close to chain A (ligand IL -19)**

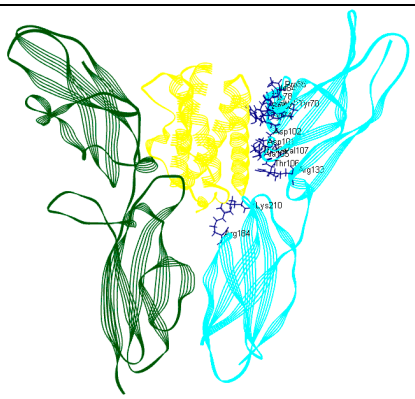

Residues of chain βB (receptor IL-20βB) close to chain A (ligand IL- 19)

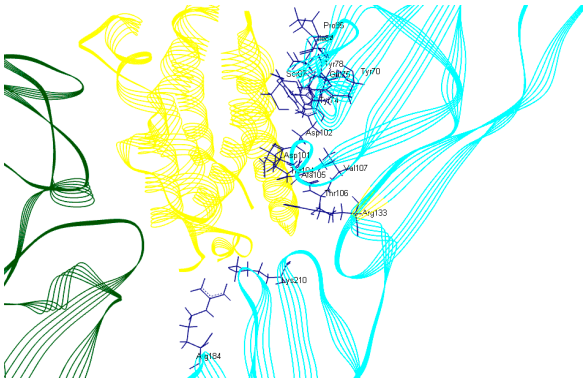

Zoomed in view of residues of chain βB (receptor IL-20βB) close to chain A (ligand IL- 19)

Table S4: List of inter-chain interacting residues within model A

Non-bond Monitor 1			
B:TYR70:OH - A:ARG84:NE	B:LYS210:HZ2 - A:ASP15:OD1	B:LYS210:HE1 - A:ASP15:OD1	A:ALA147 - R:LEU133
B:TYR74:OH - A:PHE72:O	R:ARG128:HH21 - A:ASP34:OD2	R:GLY77:HA1 - A:ASN38:O	A:ALA159 - R:PRO223
B:VAL107:CG1 - A:ASN91:ND2	R:ARG128:HH22 - A:ASP34:OD2	R:GLY77:HA2 - A:THR40:OG1	B:TYR70 - A:ARG84
B:VAL107:CG1 - A:ASN91:HD21	R:ARG128:NH1 - A:ASP143:OD2	R:TRP194:HA - B:PRO189:O	B:TYR74 - A:ALA90
B:VAL107:HG11 - A:ASN91:HD21	A:LYS27:NZ - R:GLU134:OE2	R:GLY224:HA1 - A:SER157:OG	B:TYR78 - A:LYS73
B:VAL107:HG12 - A:ASN91:ND2	A:ARG84:NH1 - B:ASP102:OD1	A:HIS17:HD2 - R:GLY224:O	R:TYR130 - A:ALA147
B:VAL107:HG12 - A:ASN91:HD22	A:ARG84:NH2 - B:ASP102:OD2	A:HIS18:HE1 - B:THR104:O	R:TRP194 - B:VAL153
R:PHE74:CZ - A:ASN38:OD1	A:LYS151:NZ - R:GLU105:OE2	A:ARG84:HD2 - B:ASP101:O	R:TRP207 - B:PRO197
R:PHE74:CE1 - A:ASN38:OD1	B:HIS191:HN - R:SER195:O	A:ARG84:HD2 - B:ASP102:O	A:HIS17 - R:PRO226
R:PHE74:HZ - A:ASN38:OD1	R:TYR76:HH - A:VAL39:O	A:SER88:HB1 - B:THR104:OG1	
R:TYR130:OH - A:ALA147:CB	R:TYR76:HH - A:GLU141:OE2	B:HIS151 - R:TRP194	
R:GLY224:N - A:ALA159:CB	R:ARG128:HH12 - A:GLY140:O	B:HIS191 - R:TRP194	
R:GLY224:N - A:ALA159:HB2	R:ASN187:HD21 - B:ASP148:OD1	B:HIS191 - R:TRP194	
R:GLY224:HN - A:ALA159:CB	R:SER195:HN - B:PRO189:O	B:PHE150 - R:TRP207	
R:GLY224:HN - A:ALA159:HB2	A:ASN38:HD22 - R:GLN78:O	R:TRP207 - B:PHE150	
R:GLY224:HN - A:ALA159:HB3	A:ARG84:HH21 - B:TYR70:OH	B:ILE84 - A:LEU83	
R:PRO225:HD2 - A:GLU20:OE1	A:ARG84:HH21 - B:PRO85:O	B:PRO85 - A:PRO80	
A:ARG84:HE - B:TYR70:OH	B:VAL190:HA - R:SER195:O	A:PRO80 - B:ILE84	
B:LYS210:HZ2 - A:ASP15:OD1	B:LYS210:HE1 - A:ASP15:OD1	A:ALA147 - R:LEU133	